Available online at www.sciencedirect.com
ScienceDirect
Journal of Catalysis 250 (2007) 102–109
JOURNAL OF CATALYSIS
www.elsevier.com/locate/jcat

# Photoelectrocatalytic oxidation of organic compounds at nanoporous $TiO_2$ electrodes in a thin-layer photoelectrochemical cell

Huijun Zhao *, Dianlu Jiang, Shanqing Zhang, William Wen

*Griffith School of Environment, Gold Coast Campus, Griffith University, PMB 50, Gold Coast Mail Centre, QLD 9726, Australia*

Received 4 March 2007; revised 18 April 2007; accepted 22 May 2007

Available online 29 June 2007

**Abstract**

A simple, rapid, and effective photoelectrochemical method is proposed to quantitatively characterise photocatalytic degradation behaviour of organic compounds at nanoporous $TiO_2$ film electrodes in a thin-layer photoelectrochemical cell. This method uses the charge obtained by integrating the photocurrent originating from the photocatalytic oxidation of organic compounds to quantify the extent of degradation. Complete mineralisation was observed for all organic compounds investigated. A double-exponential kinetic rate expression was acquired using a computer simulation method, indicating two simultaneous kinetic processes. Photocurrent profiles of different organic compounds complied well with the proposed theoretical model. Both pre-exponential and exponential constants were obtained. The rate of the fast kinetic component is 10–25 times faster than that of the slow kinetic component. It was found that the identities of organic compounds have no significant effect on the photocatalytic oxidation kinetics, whereas the availability of the organic compounds to capture photoholes plays a decisive role.
Crown Copyright © 2007 Published by Elsevier Inc. All rights reserved.

*Keywords:* Porous $TiO_2$; Photocatalysis; Photoelectrochemistry; Thin-layer photoelectrochemical cell

## 1. Introduction

Up to now, $TiO_2$ has been the dominant semiconductor photocatalyst, although many other types of semiconductor photocatalysts are available [1–4]. The domination of $TiO_2$ in the field can be attributed to its superior photocatalytic oxidation ability and nonphotocorrosive, nontoxic, and inexpensive characteristics. $TiO_2$ can be readily synthesized in its highly photoactive nanoparticle forms [1–3]. To date, much research effort has been devoted to understanding the fundamental processes of $TiO_2$ photocatalysis in attempt to improve photocatalytic efficiencies [2–8]. Nevertheless, much of the published data has been obtained from bulk reactors (cells) of slurry and immobilised $TiO_2$ photocatalytic systems [1–4,8–11]. In practice, the use of a thin-layer reactor can improve the photoefficiency because of enhanced mass transfer and reduced UV absorption by the aqueous medium. In this regard, the investigation of photocatalysis processes in thin-layer reactors is of particular interest to the researchers in the field.

In a bulk reactor (cell), the reaction is often nonexhaustive, and the ratio between the volume of the solution and the electrode area is large. Consequently, the change in the substrate concentration in the bulk solution is negligible during the reaction [12,13]. For this reason, a steady-state mass transfer condition can be achieved, and a limiting (steady-state) photocurrent can be attained. The relationship between the current and the substrate concentration can be obtained mathematically by solving the differential equations of Fick's law using a set of identified semi-infinite boundary conditions [14]. Nevertheless, the circumstance in a thin-layer cell is very different from that of a bulk cell. First, the ratio between the solution volume and the electrode area is very small, which makes the substrate concentration in the bulk solution decrease rapidly once the reaction begins. As a result, the steady-state mass transfer condition cannot be sustained, and a limiting current cannot be attained. Second, the semi-infinite boundary conditions are invalid for a thin-layer cell process, because the thickness of the concentration depletion layer is limited by the thickness of the cell ($<200$ μm) [14,15]. Thus, the mathematical treatment of a

* Corresponding author. Fax: +61 7 5552 8067.
*E-mail address:* h.zhao@griffith.edu.au (H. Zhao).

0021-9517/$ – see front matter Crown Copyright © 2007 Published by Elsevier Inc. All rights reserved.
doi:10.1016/j.jcat.2007.05.013

thin-layer system is quite different from that of a nonexhaustive degradation mode in a bulk reactor [14,15]. The present work aimed to investigate the characteristics of exhaustive photoelectrocatalytic degradation of organics in a thin-layer cell. In particular, the investigation focused on quantifying the extent of the degradation and expressing the kinetics of the exhaustive degradation processes.

Although the photocatalytic degradation of a wide spectrum of organic compounds has been extensively investigated [16–18], a method to provide simple, rapid, and accurate quantification of the extent of photocatalytic degradation has not yet been realised. Most of current methods quantify the extent of the degradation by measuring the amount of original compound that disappeared. Under these conditions, extra caution must be taken in data interpretation, because the photocatalytic degradation of organic compounds (even the simplest ones, such as formic and oxalic acids) will take a few steps and involve intermediates [16,19]. In fact, the amount of the original compound disappearance can be used to represent the extent of the degradation only under the situation in which the final degradation products are accurately known. In addition, for these methods, the accuracy of the measurement is questionable due to the complicated experimental procedures involved [12,13,20,21].

The kinetics of $TiO_2$ photocatalysis has been extensively investigated [10,11,22–24]. Recent systematic studies have provided much meaningful insight into the kinetic characteristics of the $TiO_2$ photocatalytic processes [25–30]. A Langmuir–Hinshelwood kinetic model [27–29], a two-site kinetic model [25,26], and a newly proposed kinetic model [30] were used in these studies. These kinetic models are applicable to describe the kinetics of a photocatalytic process under equilibrium or pseudo-steady-state conditions. The measured kinetic parameters tend to be apparent rather than inherent, however. With these methods, the rate of disappearance of the target organic compound was used almost exclusively to represent the reaction rate. As a result, the information regarding the extent (percentage) and degree (final products) of oxidation becomes necessary and must be taken into account for interpretation of the obtained kinetics data. This is because the oxidation of different organic compounds requires transferring different numbers of electrons, and even for the same organic compound, different degrees of oxidation require transferring different numbers of electrons.

It is apparent that existing methods are unsuitable for studying the kinetics of a photocatalytic process in thin-layer reactors. In this work, we propose a new photoelectrochemical method to quantify the kinetic characteristics based on a similar principle of measurement as described previously [21,31]. Because a photocatalytic degradation process is essentially an electron-transfer process, the rate of the electron captured from organic compound can be considered an inherent property of a photocatalytic system, which can be used to best represent the photocatalytic activity and photoefficiency [21]. For this reason, a photoelectrochemical method based on measuring the total amount of photoelectrons generated from the photocatalytic oxidation of organics is used to quantify the extent and the degree of the degradation, in accordance with the Faraday's law. The use of charge to express the degradation process can greatly minimise (if not completely eliminate) the effect of many interfering factors of the solution processes (e.g., the rate of mass transfer) and interfacial processes (e.g., adsorption). In addition, the rate of electron-capturing (photocurrent) can be used to describe the kinetics of photocatalytic degradation process in the thin-layer cell. The ability to investigate the degradation kinetics of organic mixtures is a unique advantage of the proposed method. Because the degradation mechanism and reaction kinetics are strongly influenced by the adsorption properties of the organic compound [32], two groups of model compounds were chosen for the investigation: a strong adsorbate (e.g., carboxylic acid) and a weak adsorbate (e.g., aliphatic alcohol).

## 2. Experimental

### 2.1. Materials

Indium tin oxide (ITO) conducting glass slides (8 Ω/square) were supplied by Delta Technologies Limited. Titanium butoxide (97%, Aldrich), potassium hydrogen phthalate (AR, Aldrich), formic acid (AR, Aldrich), oxalic acid (AR, Ajax Chemicals), succinic acid (99%, Sigma), malonic acid (Sigmaultra, Sigma), methanol (99.8%, BDH), D-glucose (99%, BDH), salicylic acid (AR, Aldrich), sodium acetate (AR, Ajax), phenol (99%, Sigma), phenylalanine (99%, Sigma), sodium nitrite (AR, Aldrich), 4-chlorophenol (99%, Aldrich), acetone (AR, Aldrich), phenol (99%, Sigma), and glutaric acid (99%, Sigma) were used as received. All other chemicals were of analytical grade and purchased from Aldrich unless stated otherwise. All solutions were prepared using high-purity deionised water (18 MΩ cm; Millipore Corp.).

### 2.2. Preparation of the nanoporous $TiO_2$ film electrode

Aqueous $TiO_2$ colloid was prepared by the hydrolysis of titanium butoxide according to the method described by Nazeeruddin et al. [33]. The resultant colloidal solution contains 60 g $dm^{-3}$ of $TiO_2$ solid with particle sizes of 8–10 nm. Carbowax (30%, w/w based on the solid weight of the $TiO_2$ colloid) was added to increase the porosity of the final $TiO_2$ film. The colloid thus obtained was used for the fabrication of $TiO_2$ nanoporous film. ITO slides were used as the conducting substrate. Details of the ITO pretreatment were given in our previous publication [12]. After the pretreatment, the ITO slide was dip-coated in the $TiO_2$ colloidal solution. The coated electrodes were then calcined in a muffle furnace at 700 °C for 16 h in air.

The surface morphology of the film was examined by scanning electron microscopy (SEM), which revealed a rough and porous film surface [31]. Crystallite size of 30–50 nm was observed, indicating that the particles are sintered aggregates from primary nanoparticles (8 nm). X-ray diffraction (XRD) analysis was used to identify the crystalline phase of the $TiO_2$ film. It revealed that the resultant $TiO_2$ film was a mixture of anatase (96.8%) and rutile (3.2%) [31]. The ratio of the two different

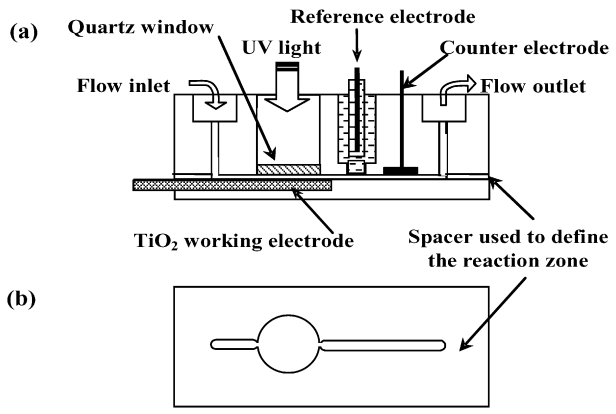


Fig. 1. The schematic diagram of the thin-layer photoelectrochemical cell.

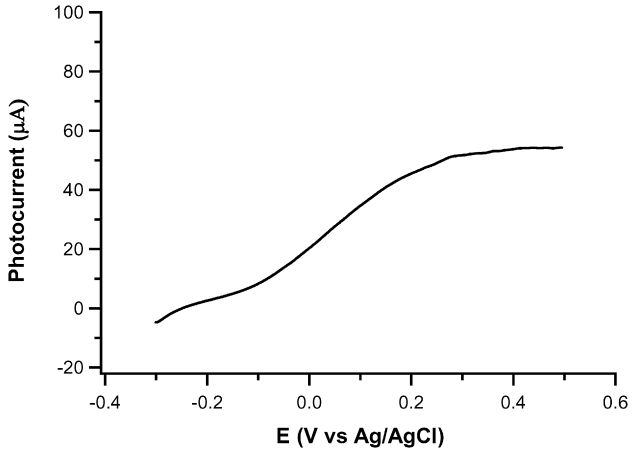


Fig. 2. Linear potential sweep voltammogram of a $TiO_2$ porous film electrode in 2.0 M $NaNO_3$ solution in the photoelectrochemical thin-layer cell under UV illumination.

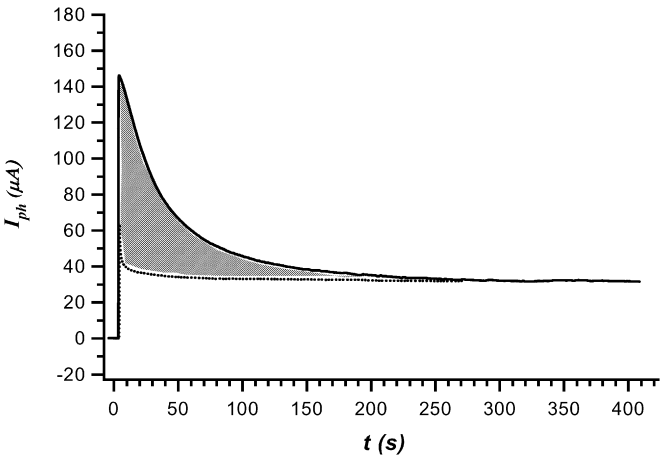


Fig. 3. Typical photocurrent responses obtained from the thin-layer cell. 2.0 M $NaNO_3$ (dash line) and 2.0 M $NaNO_3$ plus 100 μM potassium hydrogen phthalate (solid line).

crystal forms was calculated in accordance with the peak intensity ratio of $I_A(101)/I_R(110)$. The average crystallite size of the mixed-phase film was ca. 33 nm, which was also calculated from XRD peak broadening of the anatase (101) plane using Scherrer's equation [31].

### 2.3. Apparatus and methods

All photoelectrochemical experiments were performed at 23 °C in a three-electrode thin-layer photoelectrochemical cell with a quartz window for illumination (see Fig. 1a). The $TiO_2$ film electrode was used as a working electrode, with the area defined by an aperture of a 0.65-$cm^2$ spacer window (Fig. 1b). The thickness of the spacer was 200 μm, which defined a cell volume of 13.0 μL. A saturated Ag/AgCl electrode and a platinum mesh were used as the reference and auxiliary electrodes, respectively. A voltammograph (CV-27, BAS) was used for application of potential bias in photoelectrolysis experiments and linear potential sweep experiments. Potential and current signals were recorded using a Macintosh computer (7220/200) coupled to a Maclab 400 interface (AD Instruments). Illumination was carried out using a 150 W xenon arc lamp light source with focusing lenses (HF-200w-95, Beijing Optical Instruments). To prevent heating of the sample solution by the infrared light, the light beam was passed through an UV bandpass filter (UG 5, Avotronics Pty. Limited) before the electrode surface was illuminated. The light intensity was 6.6 mW/$cm^2$, as measured with a UV irradiance meter (UV-A Instruments of Beijing Normal University).

## 3. Results and discussion

### 3.1. Photocurrent–potential responses

For a thin-layer cell, the solution resistance is high due to the thin solution channel between the working and the reference electrodes, which could generate significant IR drops, leading to the deformation of current–potential responses. To avoid this, a high concentration electrolyte (i.e., 2.0 M $NaNO_3$) was used. Fig. 2 shows a typical linear potential sweep voltammogram of a porous $TiO_2$ film electrode in 2.0 M $NaNO_3$ under illumination. No distortion in photocurrent potential responses were observed, indicating that the 2.0 M supporting electrolyte is sufficient. In fact, the photocurrent potential characteristics observed were similar to those of the electrode in a conventional bulk cell [20,21]. As shown in Fig. 2, in the low potential range, the photocurrent increased with potential bias, indicating that electron transport across the film was the limiting step of the overall process [20,21,34]. The photocurrent saturation at higher potential ($> +0.3$ V) is because the overall process was dominated by the electron capturing rate at the $TiO_2$–solution interface [20,21,34]. To obtain a photocurrent response that represents the rate of electron capture at the interface without the influence from the electron transport across the photocatalyst film, a potential bias of +0.30 V was subsequently adopted for all experiments [20,21,34].

### 3.2. Measurement of transient photocurrent and charge

Fig. 3 shows the transient photocurrent decay of the electrode in a 2.0 M $NaNO_3$ solution with and without potassium hydrogen phthalate (KHP) in the thin-layer cell. With the blank

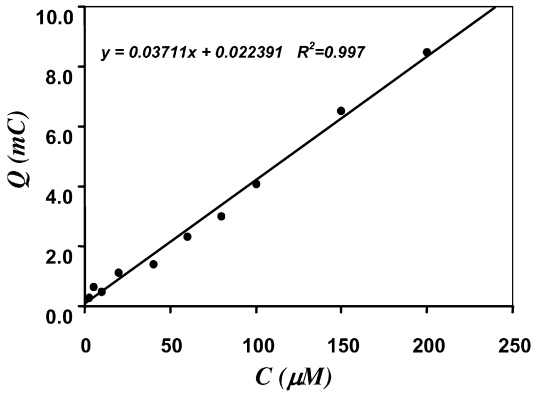


Fig. 4. A plot of net charge against the initial potassium hydrogen phthalate concentration.

electrolyte solution, a smaller photocurrent response spike (dotted line) is observed, which is attributed to photocatalytic oxidation of water. In the presence of KHP, the photocurrent spike (solid line) increased due to photocatalytic oxidation of both the organic compound and water. After depletion of the organic compound concentration in the reaction zone, the photocurrent decayed to a steady photocurrent due purely to the photocatalytic oxidation of water. The net charge originating from photocatalytic degradation of organic compound can be measured by the charge difference between the two cases [21]. Note that this net charge can be quantitatively converted to the equivalent amount of organic compound being oxidised, in accordance with Faraday's law [21]. Also note that the net photocurrent due purely to the photocatalytic oxidation of organics also can be obtained by deducting the black photocurrent from the overall photocurrent. Under the experimental conditions of this study, this net photocurrent can be used to represent the instant rate of photohole capture process at the interface, which should be the limiting step of the overall process [20,21,34].

### 3.3. Stoichiometry of photocatalytic degradation

First, the photocatalytic degradation of KHP was investigated. The stoichiometric oxidation of KHP can be represented as

$$C_8H_6O_4 + 12H_2O \rightarrow 8CO_2 + 30H^+ + 30e^-. \quad (1)$$

That is, the mineralisation of 1 mol of KHP requires 30 mol of electrons. Consequently, Faraday's law can be written as

$$Q = 30FCV = kC, \quad (2)$$

where $Q$ is the theoretical net charge, $V$ is the volume of the thin-layer cell, $F$ is the Faraday constant, and $C$ is the initial concentration of the organic compound.

According to Faraday's law, if the complete mineralisation of KHP has been achieved, then the relationship between the net charge and the concentration should be linear and with a theoretical slope ($k$) of 0.03763 (mC/μM), where the cell volume, $V = 13$ μL, is used. Fig. 4 shows the plot of the net charge against the concentration. A linear relationship with an experimental slope value of 0.03711 (mC/μM) was obtained. This indicates that >98% of KHP in the sample has been completely mineralised to $CO_2$.

Table 1
Number of electrons ($n$) required for complete mineralisation of different compounds

| Compounds | $n$ | Compounds | $n$ | Compounds | $n$ |
|---|---|---|---|---|---|
| Methanol | 6 | *p*-Chlorophenol | 26 | Malonic acid | 8 |
| Glucose | 24 | Glycin | 6 | Succinic acid | 14 |
| Phthalic acid | 30 | Oxalic acid | 2 | Glutaric acid | 20 |

Table 2
Molar composition of mixture 1 and mixture 2

| Mixture 1 (mol%) | | Mixture 2 (mol%) | |
|---|---|---|---|
| Phthalic acid | 10% | Phthalic acid | 20% |
| Salicylic acid | 10% | Phenol | 20% |
| Glucose | 10% | Glucose | 20% |
| Phenol | 10% | Methanol | 20% |
| Methanol | 20% | Malonic acid | 20% |
| Acetone | 20% | | |
| Acetic acid | 20% | | |

Considering that the experimental net charge used in Fig. 4 was obtained by simple subtraction of the background charge (due to the photocatalytic oxidation of water) from the overall charge (due to the photocatalytic oxidation of both water and organics), the excellent linear relationship shown in Fig. 4 implies that the rate of photocatalytic oxidation of water does not change with the concentration of organic compounds. This is a very interesting finding, because the KHP is known to be a strong adsorbent [34], and an increase in KHP concentration certainly will result in a decreased surface coverage of water, which normally would lead to a decreased rate of water oxidation that underestimates the proposed method. But this did not happen, as evidenced by the experimental observation, which may be explained by a two-site kinetic model [25,26].

The extent of oxidation of other organic compounds was subsequently investigated using the aforementioned method. The stoichiometric photocatalytic mineralisation of organic compounds can be generally represented as

$$C_yH_mO_jN_kX_q + (2y - j)H_2O \rightarrow yCO_2 + qX^- + kNH_3 + (4y - 2j + m - 3k)H^+ + (4y - 2j + m - 3k - q)e^-, \quad (3)$$

where N and X represent nitrogen and halogen, respectively. The numbers of carbon, hydrogen, oxygen, nitrogen, and halogen atoms in the organic compound are represented with $y$, $m$, $j$, $k$, and $q$, respectively.

The number of electrons ($n$) required for complete mineralisation of the organic compound can then be given as

$$n = 4y - 2j + m - 3k - q. \quad (4)$$

Table 1 lists the organic compounds used for this study and the number of electrons required for complete mineralisation of each organic compound.

To evaluate the applicability of our method, we also investigated the mixture solutions containing different organic compounds. Table 2 provides compositions of the mixture solutions.

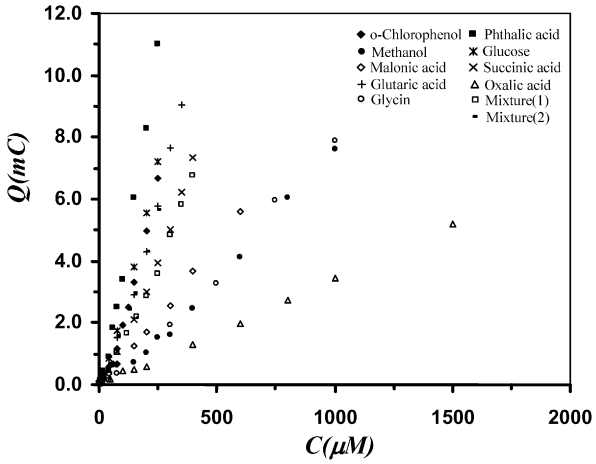


Fig. 5. A plot of net charge against the initial molar concentration for different compounds.

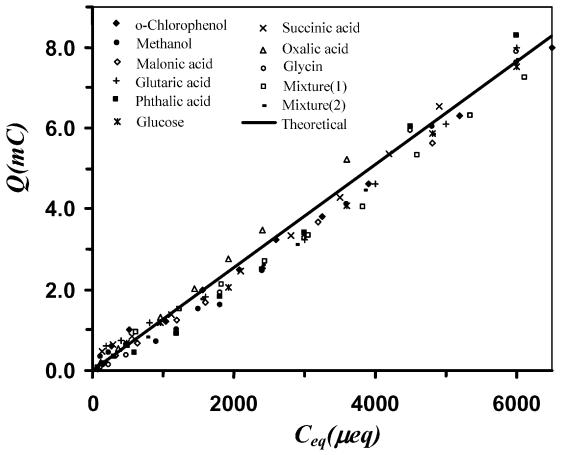


Fig. 6. A plot of net charge against the initial equivalent concentration for different compounds.

Fig. 5 shows the plot of measured net charge ($Q$) versus molar concentration ($C_M$) for different organic compounds and the mixture solutions. As was shown in Fig. 4, linear relationships between the net charge and the substrate concentration were obtained for all cases investigated. As expected, the slope ($k$) value obtained from individual case was markedly different due to the differences in the number of electrons required for complete mineralisation of 1 mol of individual organic compound. The experimental slope of each organic compound including the two mixture solutions was measured against their theoretical slope value; it was found that the experimental slope values for all cases investigated were within 97.5–101% of the theoretical slope values. Considering the experimental errors and the purity of the reagents, it is reasonable to claim that complete mineralisation was achieved for all cases.

The extent of oxidation for different organic compounds also can be evaluated collectively by introducing equivalent concentration, $C_{eq}$, which is defined as the molar concentration ($C_M$) multiples the number of electrons ($n$) required for complete mineralisation, that is, $C_{eq} = n \cdot C_M$. The physical meaning of this concentration unit is that the electron demands for complete mineralisation of different organic compounds with a given $C_{eq}$ are the same regardless of their identities, molecular sizes, and chemical structures. In other words, this unit conversion normalises the molar concentration into a noncharacteristic concentration. With such a concentration unit, Faraday's law can be given as

$$Q = nFVC_M = FVC_{eq}. \quad (5)$$

That is, for different organic compounds, if complete mineralisation is achieved, then a plot of the net charge against the $C_{eq}$ for all organic compounds should fit into a single straight line with a unity slope of $k = FV = 1.254 \times 10^{-3}$ mC/μEq. Fig. 6 shows the $Q/C_{eq}$ relationships for different organic compounds. All compounds investigated can be fit into a straight line. The experimental slope value obtained from the line of the best fit was $1.225 \times 10^{-3}$ mC/μEq (with $R^2 = 0.986$), which is almost identical to the theoretical slope value, indicating complete mineralisation of all organic compounds. The data distribution along the theoretical line were slightly different for different compounds due to the edge effect differences, because for a given equivalent concentration, the corresponding molar concentration of different compounds can be 15 times different.

Further experiments were carried out to examine the situation with different organic compounds coexisting in a sample solution. Two different mixture solutions containing different organic compounds were used for this investigation (see Table 2). The calculated noncharacteristic electron transfer numbers ($n$) for mixture solutions (1) and (2) were 17.0 and 19.2, respectively, assuming that all organic components in the sample were completely mineralised. As shown in Fig. 6, the $Q/C_{eq}$ relationships obtained for both mixture solutions were almost identical to those obtained from single organic compound solutions, indicating that all organic components were fully oxidised and that the coexistence of different organic compounds does not affect the photocatalytic degradation process under exhaustive degradation conditions.

### 3.4. Kinetics of photocatalytic degradation in thin-layer cells

The kinetic rate expression can be mathematically obtained if a set of appropriate boundary conditions can be defined. Nevertheless, defining the boundary conditions for a given reaction system leading to an exact mathematic solution can be difficult, especially with a thin-layer cell, in which the boundary conditions depend on geometry and dimension of both the working electrode and the cell [15]. To avoid this problem, for this study, a computer simulation method was used to obtain the kinetic rate expression.

Under the experimental conditions used in this study, the overall reaction is under the control of interfacial photohole capture process [20,21,34]. Therefore, the photocurrent ($I_{ph}$) obtained represents the instant rate of photohole capture, which in turn represents the instant rate of the overall photocatalytic oxidation [20,21,34]. This provides a base for obtaining the kinetic rate expression from photocurrent profiles. In this study, photocurrent profiles obtained from the thin-layer cell for all

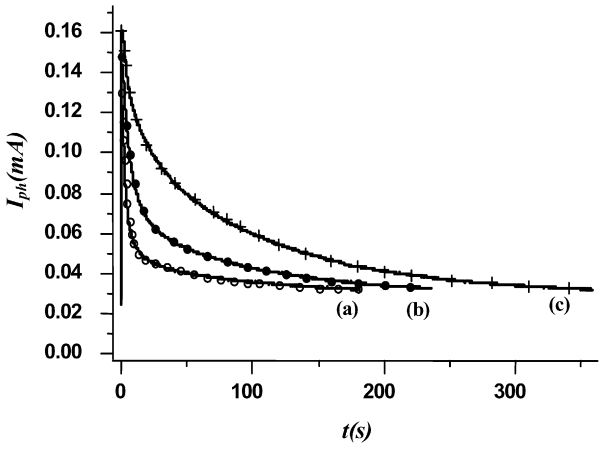


Fig. 7. Experimental photocurrent decay profiles and fitting curves: (a) 20, (b) 80, (c) 200 μM of sodium hydrogen succinate.

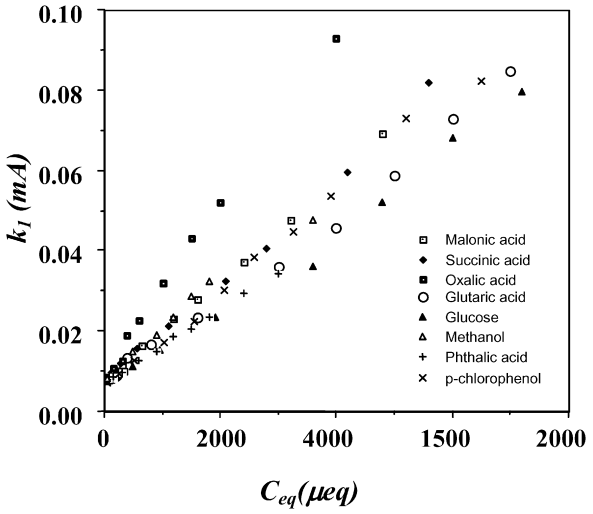


Fig. 8. A plot of $k_1$ against equivalent concentrations for different compounds.

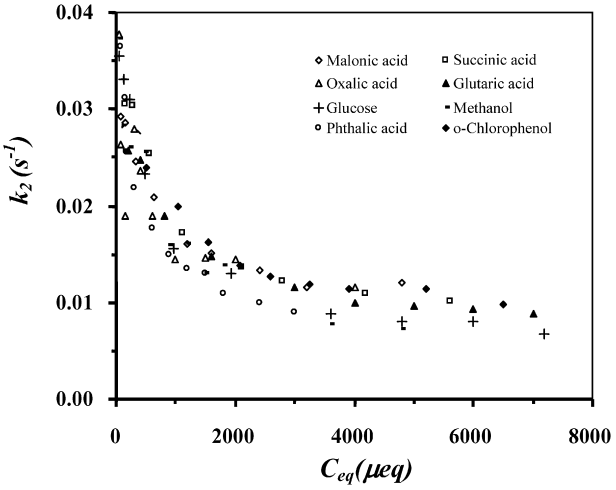


Fig. 9. A plot of $k_2$ against equivalent concentrations for different compounds.

organic compounds investigated were found to be smoothly decayed with time (Fig. 3). All photocurrent profiles obtained from a wide range of substrate concentrations can be fitted to a double-exponential expression,

$$I_{\mathrm{ph}} = I_0 + k_1 \exp(-k_2 t) + k_3 \exp(-k_4 t). \quad (6)$$

Fig. 7 shows a set of typical curve-fitting results. It can be seen that the experimental curves fit well with Eq. (6). The double-exponential photocurrent decay implies that two kinetic processes occur simultaneously during the photocatalytic degradation of organic compounds in the thin-layer photoelectrochemical cell. In Eq. (6), $I_0$ is a constant, and its value is independent of the type of organics and concentrations, which can be assigned to the photocatalytic oxidation of water. $k_1$ and $k_3$ are the pre-exponential factors, the values of which should change with the initial concentration in the cell and the quantity of organic compounds at the electrode surface. The absolute values of $k_1$ and $k_3$ represent the instantaneous initial rate of reaction; $k_2$ and $k_4$ are the exponential decay constants or rate constants.

The pre-exponential constant $k_1$ varied linearly with initial molar concentration for all organic compounds investigated. The slopes of different organic compounds differed greatly due to the different numbers of electrons transferred. But plotting $k_1$ against $C_{\mathrm{eq}}$ (nonspecific concentration) showed significantly reduced differences in the slope values among different organics as the differences in electron number were normalised (Fig. 8), indicating that the chemical structure of the organic compounds has little influence on the initial reaction rate of the first kinetic component. It can be seen from Fig. 8 that the slope for oxalic acid at concentrations >500 μEq is higher than that of all other organics, due to the current doubling effect [21,35]. It also can be seen that a common intercept appears for all cases, due to the photocatalytic oxidation of water.

For a given organic compound, the exponential decay constant, $k_2$, was found to initially decrease with concentration, then reach a constant value at high concentration range. The values of $k_2$ for different compounds were dramatically different at the same initial molar concentration. When the concentrations were normalised to nonspecific concentrations, $C_{\mathrm{eq}}$, the values of $k_2$ obtained were very close for all organic compounds investigated and with the same variation trends shown in Fig. 9. This indicates that the photohole demand is a decisive factor in the kinetics of photocatalytic degradation of organic compounds. If photohole supply (proportional to the light intensity) is sufficient for the photohole demand, then the chemical identity of an organic compound has little influence on the photocatalytic degradation kinetics.

The constant $k_3$ is the pre-exponential factor for the fast photocatalytic process. Fig. 10 shows the plot of $k_3$ against $C_{\mathrm{eq}}$ for different organic compounds. As shown, the weak adsorbates and strong adsorbates exhibited very different behaviours. For the weak adsorbates (e.g., methanol, glucose, *p*-chlorophenol), $k_3$ values were virtually independent of concentration and smaller than those of the strong adsorbates. In contrast, for strong adsorbates (e.g., phthalic acid, oxalic acid, malonic acid, succinic acid, glutaric acid), the $k_3$ values were largely dependent on the concentration. Plotting the $k_3$ against the $C_{\mathrm{eq}}$ gives similar trends of variations for all strong adsorbates. For these strong adsorbates, the $k_3$ initially increased

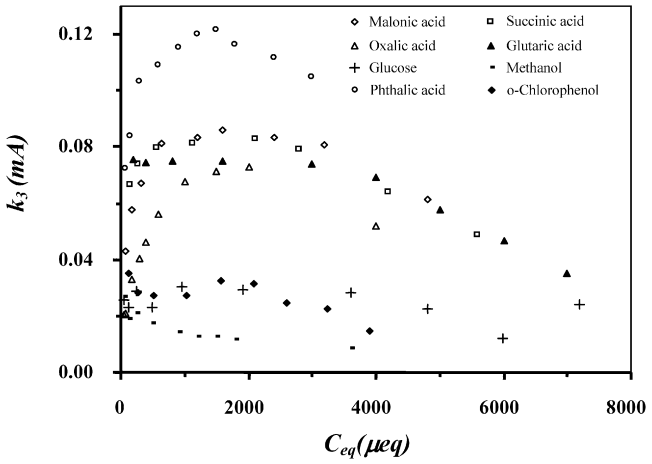


Fig. 10. A plot of $k_3$ against equivalent concentrations for different compounds.

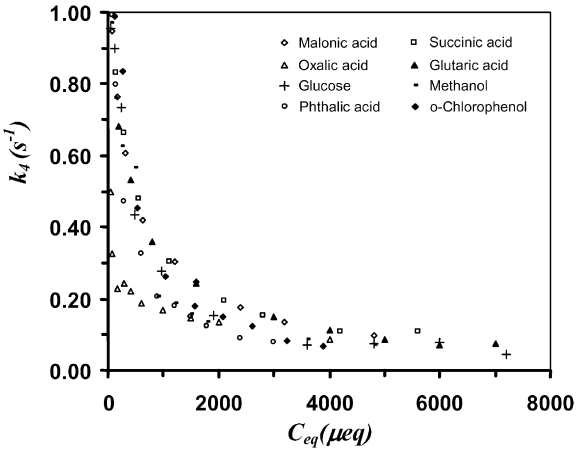


Fig. 11. A plot of $k_4$ against equivalent concentrations for different compounds.

with concentration and reached a maximum, then decreased in the high concentration range. The peak concentrations for different compounds were slightly different, varying from 1400 to 2000 μEq. Clearly, the value of $k_3$ is related to the amount of the surface adsorption. The increase in the value of $k_3$ at low concentration was due to the increased amount of surface adsorption. However, the decrease in the value of $k_3$ at high concentration range was not caused by decreased adsorption; rather, it was due to the accumulation of the adsorbed substrate and/or its intermediates. Similar trends of variation of $k_3$ with the same $C_{eq}$ for different strong adsorbates again suggest that the total photohole demand is a decisive factor.

The constant $k_4$ is the fast exponential decay constant. Fig. 11 shows the plot of $k_4$ against $C_{eq}$ for different organic compounds. It can be seen that the trends of variation are almost identical to those obtained in Fig. 9 for $k_2$, suggesting the total photohole demand (rather than chemical identities of organic compounds) is the decisive factor in the photocatalytic degradation kinetics. It also can be seen that $k_4$ values are 10–25 times larger than the $k_2$ values of a organic compound at corresponding concentrations, indicating that the kinetic rate for the second exponential component is faster than that for the first exponential component. It should be noted that as the concentration increased, $k_4$ gradually decreased and approached the value of the slow exponential decay constant, $k_2$, at very high concentrations.

## 4. Conclusion

The experimental results show that our proposed photoelectrochemical method is a simple, rapid, and effective approach to quantitative studies of the photocatalytic degradation behaviour of organic compounds on nanoporous $TiO_2$ film electrodes in a thin-layer photoelectrochemical cell. The rate of water photocatalytic oxidation is independent of the type and concentration of organic compounds present. Photoelectrochemical quantification of the extent of degradation of different organics and their mixtures found that complete mineralisation was achieved for all cases investigated. A double-exponential kinetic rate expression was obtained by computer-fitting the experimental photocurrent profiles. The common intercept represents the photocatalytic oxidation of water. The slow exponential decay component indicates a slow photocatalytic process that can be assigned to interfacial kinetics-related reaction processes. The rate of the slow kinetic process is similar for different electron donors. The pre-exponential constant, $k_1$, is directly proportional to the substrate concentration. Except for oxalic acid in the high concentration range, all other organic compounds have similar $k_1$ values at a given equivalent concentration. The slow exponential constant, $k_2$, is independent of the size and chemical identities of organic compounds. The fast exponential decay component indicates a fast photocatalytic process that can be assigned to the surface-related reaction processes. The pre-exponential constant, $k_3$, depends strongly on the adsorbability of the organic compounds; nevertheless, the fast exponential constant, $k_4$, is independent of adsorbability. The values of $k_4$ are 10–25 times larger than those of $k_2$ for a organic compound at corresponding concentrations.

## Acknowledgment

Financial support was provided by the Australian Research Council and Aqua Diagnostics.

## References

[1] B. Abrams, J. Wilcoxon, Crit. Rev. Solid State Mater. Sci. 30 (3) (2005) 153.
[2] K. Hashimoto, H. Irie, A. Fujishima, Jpn. J. Appl. Phys. Part 1 44 (12) (2005) 8269.
[3] M. Fernandez-Garcia, A. Martinez-Arias, J.C. Hanson, J.A. Rodriguez, Chem. Rev. 104 (9) (2004) 4063.
[4] A.J. Frank, N. Kopidakis, J. van de Lagemaat, Coordin. Chem. Rev. 248 (13–14) (2004) 1165.
[5] Y. Nosaka, M. Kishimoto, J. Nishino, J. Phys. Chem. B 102 (50) (1998) 10279.
[6] C.S. Turchi, D.F. Ollis, J. Catal. 122 (1) (1990) 178.
[7] D.F. Ollis, H. Al-Ekabi, Photocatalytic Purification and Treatment of Water and Air, Elsevier, Amsterdam, 1993, p. 225.
[8] S.U.M. Khan, M. Al-Shahry, W.B. Ingler Jr., Science 297 (2002) 2243.

[9] A.V. Taborda, M.A. Brusa, M.A. Grela, Appl. Catal. A 208 (1–2) (2001) 419.
[10] S. Kim, W. Choi, Environ. Sci. Technol. 36 (9) (2002) 2019.
[11] R.R. Bacsa, J. Kiwi, Appl. Catal. B 16 (1998) 19.
[12] D. Jiang, H. Zhao, S. Zhang, R. John, G.D. Will, J. Photochem. Photobiol. A 156 (1–3) (2003) 201.
[13] D. Jiang, H. Zhao, Z. Jia, J. Cao, R. John, J. Photochem. Photobiol. A 144 (2–3) (2001) 197.
[14] A.J. Bard, L.R. Faulkner, Electrochemical Methods, Fundamentals and Applications, second ed., Wiley, New York, 2001.
[15] P.T. Kissinger, W.R. Heineman, Laboratory Techniques in Electroanalytical Chemistry, Marcel Dekker, New York, 1996.
[16] M.R. Hoffmann, S.T. Martin, W. Choi, D.W. Bahnemann, Chem. Rev. 95 (1995) 69.
[17] A.J. Hoffman, G. Mills, H. Yee, M.R. Hoffmann, J. Phys. Chem. 96 (13) (1992) 5546.
[18] C. Kormann, D.W. Bahnemann, M.R. Hoffmann, Environ. Sci. Technol. 25 (3) (1991) 494.
[19] A. Mills, S. Morris, R. Davies, J. Photochem. Photobiol. A 70 (2) (1993) 183.
[20] D. Jiang, H. Zhao, S. Zhang, R. John, J. Phys. Chem. B 107 (46) (2003) 12774.
[21] H. Zhao, D. Jiang, S. Zhang, K. Catterall, R. John, Anal. Chem. 76 (2004) 155.
[22] J. Cunningham, G. Al-Sayyed, J. Chem. Soc. Faraday Trans. 86 (1990) 3935.
[23] R.W. Matthews, J. Catal. 111 (1988) 264.
[24] R. Enriquez, P. Pichat, Langmuir 17 (2001).
[25] M. Lewandowski, D.F. Ollis, Appl. Catal. B 43 (4) (2003) 309.
[26] M. Lewandowski, D.F. Ollis, Appl. Catal. B 45 (3) (2003) 223.
[27] D.F. Ollis, J. Phys. Chem. 109 (6) (2005) 2439.
[28] A. Mills, J. Wang, D.F. Ollis, J. Phys. Chem. B 110 (29) (2006) 14386.
[29] A. Mills, J. Wang, D.F. Ollis, J. Catal. 243 (1) (2006) 1.
[30] C. Minero, D. Vione, Appl. Catal. B 67 (3–4) (2006) 257.
[31] D. Jiang, S. Zhang, H. Zhao, Environ. Sci. Technol. 41 (1) (2007) 303.
[32] J. Krysa, G. Waldner, H. Mest'ankova, J. Jirkovsky, G. Grabner, Appl. Catal. B 64 (3–4) (2006) 290.
[33] M.K. Nazeeruddin, A. Kay, I. Rodicio, R. Humphry-Baker, E. Muller, P. Liska, N. Vlachopoulos, M. Gratzel, J. Am. Chem. Soc. 115 (1993) 6382.
[34] D. Jiang, H. Zhao, S. Zhang, R. John, J. Photochem. Photobiol. A 177 (2–3) (2006) 253.
[35] N. Hykaway, W.M. Sears, H. Morisaki, S.R. Morrison, J. Phys. Chem. 90 (25) (1986) 6663.